Journal of Colloid and Interface Science xxx (2017) xxx-xxx

Contents lists available at ScienceDirect

Journal of Colloid and Interface Science

journal homepage: www.elsevier.com

Regular Article

Effect of surfactant concentration on the responsiveness of a thermoresponsive copolymer/surfactant mixture with potential application on "Smart" foams formulations

M.M. Soledad Lencina[a], Eugenio Fernández Miconi[a, b], Marcos D. Fernández Leyes[a], Claudia Domínguez[a, b], Ezequiel Cuenca[a], Hernán A. Ritacco[a, b, *]

[a] *Instituto de Física del Sur (IFISUR-CONICET), Av. Alem 1253, Bahía Blanca 8000, Argentina*
[b] *Departamento de Física de la Universidad Nacional del Sur, Av. Alem 1253, Bahía Blanca 8000, Argentina*

ARTICLE INFO

Article history:
Received 6 July 2017
Received in revised form 21 October 2017
Accepted 23 October 2017
Available online xxx

Keywords:
Polyelectrolyte-surfactants
Foams
Responsive foams
Surface tension
Surface rheology

ABSTRACT

Hypothesis

Previous efforts to formulate smart foams composed of mixtures of PNIPAAm, a thermoresponsive uncharged polymer, and surfactants have failed because the surfactant displaces the PNIPAAm from the liquid-air interface, removing the thermal responsiveness. We hypothesized that thermoresponsive foams could be formulated with such a mixture if a charged surfactant were used in order to anchor an oppositely charged brush-type polyelectrolyte, for which PNIPAAm could be incorporated as side chains, to the interface.

Experiments

A brush-type negatively charged co-polyelectrolyte (Cop-L) with PNIPAAm as side chains was synthetized. Its mixtures with DTAB, a cationic surfactant, in aqueous solution were characterized by dynamic light scattering, surface tension and surface compression viscoelasticity measurements, as a function of both surfactant concentration and temperature. The foam stability and its responsiveness to temperature changes were studied with a homemade apparatus.

Findings

The Cop-L/DTAB mixtures were capable of producing thermoresponsive foams but only in a very narrow surfactant concentration (c_s) range, $0.3 < c_s < 1.6$ mM. The responsiveness is due to a modification of the interfacial compression elasticity induced by conformational changes of the Polyeletrolyte/surfactant aggregates at the interface. This is possible only for $c_s < 1.6$ because higher surfactant concentrations induce the polymer collapse at all temperatures, eliminating the thermal responsiveness.

1. Introduction

Liquid foams, which are formed by the dispersion of a gas in a liquid matrix [1–3], are ubiquitous systems both in nature and in human everyday life and industry [4]. They are metastable systems that persist a certain time because the three main processes that drive the dispersion to its true thermodynamic equilibrium state, which is complete phase separation, are kinetically arrested by the presence of surface-active agents, the foam stabilizers. The three processes mentioned are *drainage* [5], the flow of liquid thorough the liquid channels between bubbles due to gravity and capillarity; *coarsening* [5], the gas flow between adjacent bubbles driven by differences in capillary pressures; and *coalescence* [6], which is due to the rupture of the liquid films. The most commonly used foam stabilizers are surfactants, however polymers, proteins, and particles, among others, can also be used. Among these, mixtures of polyelectrolytes and oppositely charged surfactants [7] present some advantages as foam stabilizers, such as the low surfactant and polymer concentrations needed to produce and stabilize the foams.

Responsive or "smart" foams are liquid foams whose stability changes when the foam is subject to an external stimuli such as magnetic or electric fields, temperature and light, among others [8–10]. The responsiveness of the foams is attained via the chemical systems used as foam stabilizers, which can respond to the external stimuli in different ways. A very nice example of this kind of system is that formulated with a photoswitchable surfactant. Chevalier et al. [11] formulated foams stabilized with AzoTab, a surfactant with an azobenzene group, that changes from cis to trans-isomer when illuminated with UV or blue light. Through quite a complex mechanism, the changes suffered by the surfactant molecules produce a dramatic modification of the stability of the foam. Other examples of these kind of system are those formulated with 12-hydroxystearic acid (12-HSA) mixed with hexanolamine [12] for which the foam responsive-

* Corresponding author at: Instituto de Física del Sur (IFISUR-CONICET), Av. Alem 1253, Bahía Blanca 8000, Argentina.
Email address: hernan.ritacco@uns.edu.ar (H.A. Ritacco)

https://doi.org/10.1016/j.jcis.2017.10.090
0021-9797/

ness is due to a structural transition of the self-assembled aggregates of 12-HSA, triggered when the temperature goes over 60 °C.

As mentioned, macromolecules can be used as foam stabilizers in the formulation of responsive foams; however, in this case, the switch of foam stability generally involves invasive methods such as changing the pH or ionic strength by adding chemicals [13,14]. PNIPAAm, a polymer, undergoes a conformational transition at a critical temperature (LCST) of about 35 °C, being in a coil conformation below this temperature and collapsing to form globules above it. Additionally, it was shown that PNIPAAm can adsorb at interfaces and transit from a fluid-like to a solid-like surface layer when the transition temperature is crossed [15,16]. Because the transition is reversible both in bulk and at the interfaces, PNIPAAm aqueous solutions were considered as candidates for the formulation of "smart" foams whose stability could be switched on/off by changing the temperature. Unfortunately, the foaming properties of PNIPAAm aqueous solutions are quite poor and the foams produced from them were found to be unstable [17], precluding its use as a stabilizing agent in foam formulations. Guillermic et al. [17] tried to overcome this problem by mixing the PNIPAAm with surfactant sodium dodecyl sulfate (SDS) in order to improve the foaming properties of the solutions. The foamability and foam stability were indeed improved, however, the thermal responsiveness of the interfacial layer was lost.

With the intention of producing a foaming system capable of responding to changes in temperature, we synthetized a copolymer based on PNIPAAm and alginate, which is a negatively charged polysaccharide (see supplementary material, SM), giving place to a negatively charged polyelectrolyte with a brush-type structure, capable of forming complexes with oppositely charged surfactants. Because the PNIPAAm are incorporated as side chains, we speculated that, when mixed with an oppositely charged surfactant molecule, the responsiveness of the system to temperature changes would be maintained and that, at the same time, the foamability properties and stability of the foams would improve. The underlying idea is that the oppositely charged surfactant should anchor the charged groups of the copolymer to the interface, maintaining the thermoresponsive PNIPAAm side chains in the interfacial region.

In this article we study a mixture of the copolymer Alg-g-PNIPAAm, hereafter called Cop-L, with the cationic surfactant dodecyltrimethylammonium bromide (DTAB). Because the responsiveness of the foam is linked to the responsiveness of the stabilizer either in bulk or at the solution-air interface, we characterized the Cop-L/DTAB mixtures at the interfaces by surface tension and surface compression viscoelasticity, and in bulk by dynamic light scattering (DLS), as a function of surfactant concentration and temperature. We found that Cop-L/DTAB mixtures are capable of producing foams whose stability can be modulated by changing the temperature, however, this can be done only for a certain surfactant concentration range. In this range, the responsiveness in the foam stability seems to be mediated by changes in surface compression elasticity when a critical temperature is crossed. The change observed in surface elasticity could be at the origin of the observed transition in the coalescence dynamics from a continuous ($T < LCST$) to a cooperative (avalanches) process ($T > LCST$). Contrary to what happens with emulsions [18], to our knowledge there has been no report in the literature of a smart foam capable of responding to changes in temperature based on PNIPAAM or its derivatives.

2. Materials and methods

2.1. Materials

The cationic surfactant, dodecyltrimethylammonium bromide (DTAB) was obtained from Sigma-Aldrich (99%) and used as received.

Sodium alginate (Mw = 198, repetitive units) is the sodium salt of alginic acid, a linear polysaccharide obtained from brown algae, it is constituted by two uronic acids, 1,4 b-D-mannuronic acid (M) and 1,4 a-L-guluronic acid (G), which constitute repetitive units forming homopolymeric (MM- or GG-blocks) and heteropolymeric sequences (MG- or GM-blocks). A low viscosity sodium alginate was purchased from Alfa Aesar with a mannuronic/guluronic ratio (M/G) estimated to be 2.2 by ^{1}H NMR according to the literature [19–21]. Poly(N-isopropylacrylamide, PNIPAAm, is a synthetic polymer that presents a low critical solution temperature (LCST) undergoing a volume phase transition when heated. At low temperatures, intermolecular hydrogen bonds between water and polar groups of PNIPAAm solubilise the polymer. Above the LCST the hydrogen bonds break and hydrophobic associations between polymer chains take place, resulting in a collapsed state. The LCST for high molar mass PNIPAAm is around 32 °C, but this critical transition temperature is a function of the molar mass and polymer concentration, among other parameters [16,22–25].

The alginate-g-PNIPAAm graft copolymer (Cop-L) was obtained by a coupling reaction between the carboxyl groups of sodium alginate and the terminal amine groups of PNIPAAm-NH_2 chains, using 1-ethyl-3-(3′-(dimethylamino) propyl) carbodiimide hydrochloride (EDC) as the coupling agent. Thus, a brush-type anionic polyelectrolyte was synthesized with Mn = 4200 g/mol PNIPAAm side chains. The synthesis and further characterization were extensively described in reference [19]. The mean molecular weight of the co-polymer was determined by static light scattering giving a value of Mw = 89.5 KDa. The number of alginate monomers, and charges, per co-polymer molecule was found to be about 300, giving a contour length of about 400 nm (We did not measure the "real" size of the polymer chains, in order to give the reader an estimate of it we performed a simple calculation: the polymer chain has about 300 monomers of alginate, each of about 1–1.5 nm in length, giving a contour length of roughly 400 nm).

Polyelectrolyte solutions were prepared by dissolution in ultrapure water (Milli-Q water purification system). Due to the limited amount of polymer available, a fixed polymer concentration (c_p) of 400 mg L^{-1} was used in the preparation of all samples.

2.2. Sample preparation protocols and measurements

Polyelectrolyte-surfactant complexes often remain trapped in non-equilibrium metastable states [26] whose characteristics depend on the history of the systems, for instance on the protocols of mixing or on the time elapsed since preparation [27–31]. Two different protocols of sample preparation were used in this work. For surface tension measurements, a concentration process was employed. First, the surface tension of a DTAB free aqueous solution of Cop-L at $c_p = 400$ mg L^{-1} was measured. Subsequently, proper amounts of the copolymer, DTAB and water were added to the previous solution in order to increase the surfactant concentration, c_s, keeping the polymer concentration, c_p constant, until the targeted concentration was achieved. The surface tension, γ, was then measured after an equili-

bration period of 60 min or more. This process was repeated until the whole range of DTAB concentration was covered.

For DLS measurements, all samples were obtained by adding equal volumes of the DTAB solution with double the desired final concentration to 800 mg L^{-1} of the Cop-L solution. Solutions were left to reach equilibrium for 24 h prior to measurement. Some DLS experiments were repeated with samples prepared following the first protocol of preparation (by concentration) and we found no significant differences in the corresponding results.

2.3. Methods

2.3.1. Surface tension and step-compression surface rheology experiments

Surface tension (γ) measurements were carried out using the sensor of a Langmuir balance (KSV NIMA) and a paper Wilhelmy plate. Experiments at room temperature were performed using a Teflon trough (10 ml of volume) while a jacketed vessel was employed for temperature-dependent measurements.

Pure water surface tension measurements were used to verify optimal paper probe quality before each experimental iteration. After the solutions were poured into the corresponding vessel, surface tension was continuously measured until a stable value was achieved. The reproducibility was ±0.2 mN m^{-1}.

Temperature dependent experiments were performed in the range of 20–55 °C, with measurements being taken every 5 °C. An approximated heating rate of 1 °C/min was used between steps. Once the required temperature was reached, samples were left to reach equilibrium for 30–60 min before surface tension determination. Temperature was controlled using an external circulating water bath (Lauda Alpha) and its value was monitored by means of a thermocouple.

Stress relaxation experiments were performed following the time evolution of the surface pressure, Π, after a sudden uniaxial in-plane compression of the interface using the KSV NIMA Langmuir Balance. Surface pressure is defined as $\Pi(t) = (\gamma_0 - \gamma)$, being γ_0 and γ the surface tension of pure water and solutions respectively. The solutions were placed in the Langmuir trough and allowed to stabilize at the temperature of measurement for one hour. The experiments were performed with a relative area (A) change of 10% ($\Delta A/A_0 = 0.1$) and a compression rate of 500 mm/min. The surface stress, $\Pi(t)-\Pi_{eq}$, being Π_{eq} the surface pressure at equilibrium, acts as a restoring force which tends to restore the system to its equilibrium state, the relaxation dynamic is, in general, well described by the sum of exponentials (or just a single exponential) [32]. We treated the Π(t) data after compression by performing an inverse Laplace transformation in order to obtain the complex surface compression modulus. Details are given in the supporting information (SM). These experiments were performed at 25 and 45 °C.

2.3.2. Dynamic Light Scattering (DLS)

The hydrodynamic radiuses of the aggregates of Cop-L/DTAB complexes were measured as a function of temperature and DTAB concentration by DLS. A Malvern Autosizer 4700 with a Series 7032 Multi-8 correlator and equipped with 20 mW laser (OBIS Coherent) operating at a wavelength (λ) of 514 nm was employed, with detection at scattering angles (θ) between 30 and 150°. The intensity auto-correlation functions were processed by the Autosizer 4700 software using either a monomodal distribution analysis (cumulants) or a non-monomodal, CONTIN, analysis [33] in order to calculate the apparent translational diffusion coefficients, D_{app}, for each scattering angle. The CONTIN method was employed when the polydispersity index (PDI) obtained from cumulants was higher than 0.7. The mean translational diffusion coefficients, D_s, were then obtained by extrapolating D_{app} to $q^2 = 0$, being q the wave vector ($q = 4\pi\, n \sin(\theta/2)/\lambda$, where n is the solvent refractive index),

$$D_{app}(q) = \langle D_s \rangle (1 + Kq^2) \tag{1}$$

Once D_s was obtained, the hydrodynamic radius, R_H, was determined from the Stokes-Einstein equation,

$$D_s = \frac{k_B T}{6\pi\eta R_H} \tag{2}$$

Being k_B the Boltzmann constant, T the temperature and η the solvent (water) viscosity. The temperature was controlled (±0.1 °C) using the device's own system (PCS 8 Temperature Controller) and an external circulating water bath (Lauda Alpha).

Occasionally along the text, we will use the word "size" when referring to the hydrodynamic radius measured by DLS, however the reader should understand this in terms of Eq. (2), i.e., the size (radii) of a compact, smooth sphere with the same translational diffusion coefficient of our aggregates and not as referring to their real size.

2.3.3. Experiments on foams

In order to evaluate the properties of foams formulated with the Cop-L/DTAB mixtures, we produced foams by means of two syringes connected through a tube of very small internal diameter (Tygon internal diameter = 1/16 in., length 10 cm) as explained in the literature [34,35]. One of the syringes was filled with the desired volumes of air, V_g, and foaming solution, V_l, in order to fix the initial liquid fraction of the foam, $\phi_{l,0} = V_l/V_{foam} = V_l/(V_l + V_g)$. The liquid and air were then transferred from one syringe to the other through the constriction given by the small cross section tube, in a series of 10 cycles. In all the experiments presented in this article $\phi_{l,0}$ was fixed to 0.25. Bubbles produced by this device had a mean radius of 70 μm. The foam so produced was then transferred to a rectangular glass cell (Hellma, OS) with a light path of 1 cm, which was placed into a homemade holder adapted to a UV–vis spectrometer of fiber–optic (Ocean optics USB2000+) as shown in Fig. 1. Solutions and cells were thermalized prior to foam production. A CCD camera (Basler, acA1300-30um) was placed in front of the cell. The light emitted by a Xenon lamp (Ocean Optics PX-2) was sent through the foam sample via a fiber-optic placed at half of the cell's height and the transmitted light intensity was collected by a second fiber-optic and measured with the UV–vis spectrometer (by integrating the whole spectrum) as a function of time (every second one spectrum was taken and saved in a computer for analysis). With this setup we simultaneously followed the foam height, the volume of liquid drained and the transmitted light intensity as a function of time (see Fig. 1).

3. Results

3.1. Equilibrium surface tension isotherms

Surface tension measurements were carried out on several aqueous solutions with increasing DTAB concentration (c_s) and a fixed Cop-L concentration, $c_p = 400$ mg L^{-1}. Measurements were performed at two temperatures, 25 °C and 45 °C. The results are shown in Fig. 2. First, it is important to note the significant drop in surface tension caused by the addition of alginate-g-PNIPAAm copolymer ($c_s = 0$),

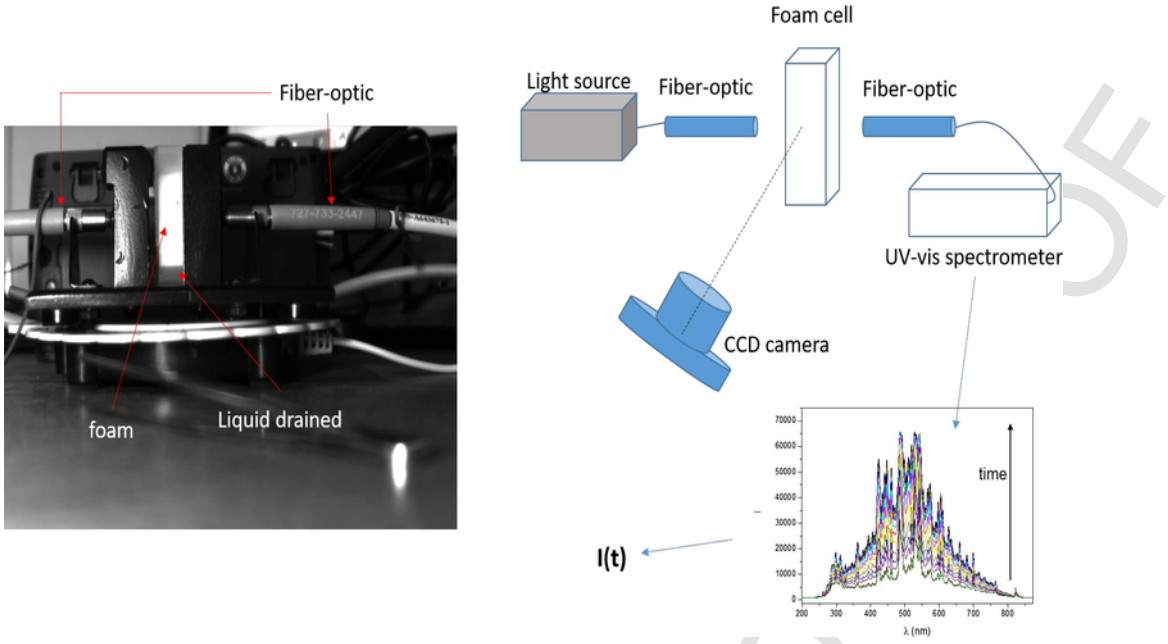

Fig. 1. Scheme of the device used to study the foams formulated with Cop_L/DTAB mixtures.

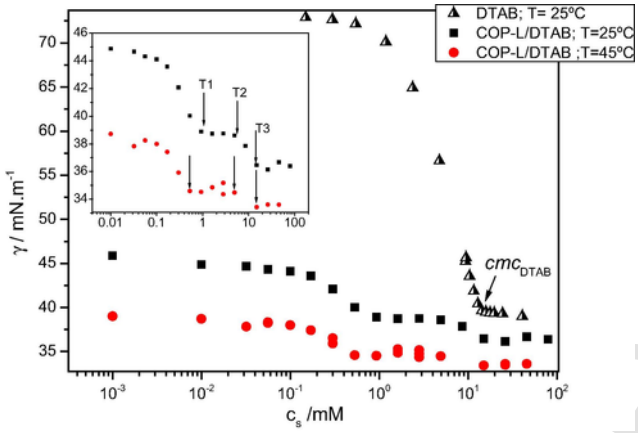

Fig. 2. Surface tension of Cop-L/surfactant mixtures as a function of DTAB concentration at 25 °C (squares) and 45 °C (circles). The surface tension isotherm for pure DTAB solutions at 25 °C are also shown (triangles). The critical micelles concentration, cmc, of DTAB is indicated in the figure (cmc ~ 15 mM at 25 °C. The cmc at T=45 °C is ~16 mM).

clearly evidencing surface activity. The surface pressure, $\Pi = \gamma_0 - \gamma$, was found to be 26.6 mN·m^{-1} and 30.2 mN·m^{-1}, at 25 °C and 45 °C, respectively.

Regarding the effect of DTAB on surface tension, Fig. 2 shows the presence of two plateaus. For the measurements at T=25 °C, the first plateau begins at a surfactant concentration of about $c_s \sim 0.7$ mM (T1 in the figure) and ends at about $c_s \sim 7$ mM (T2 in the figure). Then, as c_s increases, the surface tension drops until the second plateau begins at T3, which is about $c_s \sim 16$ mM, close to the critical micelle concentration, *cmc,* of the surfactant (*cmc* ~ 15 mM at T=25 °C). From then on, the surface tension remains constant up to the highest surfactant concentration used, $c_s \sim 80$ mM. A similar behavior is observed for T=45 °C, in this case T1 is about 0.5 mM while T2 and T3 take place at the about same concentrations.

3.2. Surface tension as a function of temperature

Fig. 3 presents the behavior of surface tension as a function of temperature for different DTAB concentrations. Surface tension values for a fixed temperature decreased with increasing DTAB concentration, as expected. For constant c_s, all solutions studied showed a linear decrease with temperature, interrupted by a notable change in slope. The intersections between lines of different slopes were found to be around 39–43 °C in all cases. These results are likely related to the presence of the low critical solution temperature (LCST) of the PNIPAAm side chains, which is LCST ~ 37 °C (see Fig. SM-4a).

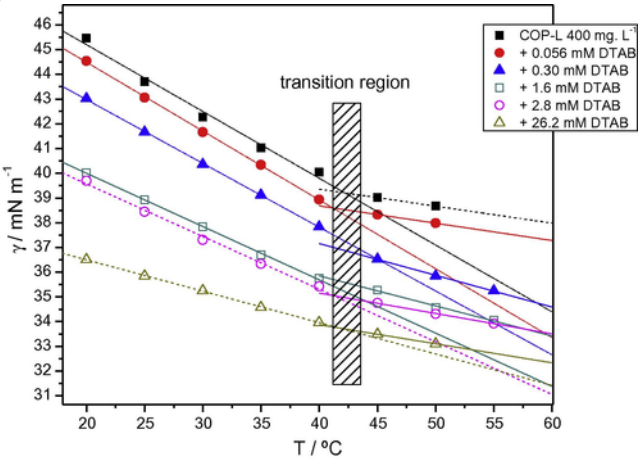

Fig. 3. Surface tension as a function of temperature for several Cop-L/DTAB mixtures with a constant polymer concentration, $c_p = 400$ mg L^{-1}. Surfactant concentrations are: $c_s = 0$ (squares); $c_s = 0.056$ mM (circles); $c_s = 0.3$ mM (triangles); $c_s = 1.6$ mM (open squares); $c_s = 2.8$ mM (open circles); $c_s = 26.2$ mM (open triangles).

3.3. Phase behavior

The phase behavior of mixed Cop-L/DTAB solutions was observed as a function of temperature and surfactant concentration. At 20 °C and for all surfactant concentrations from 0 to 30 mM the suspensions were stable and no phase separation was observed. As the temperature was increased from 20 to 55 °C, phase separation was observed for surfactant concentrations between 8 and 15 mM when the LCST was crossed. Below and above this concentration range the systems remained stable (no precipitate) at all temperatures.

3.4. Dynamic Light Scattering(DLS): Hydrodynamic radius of aggregates

In order to obtain information on the change in the size of the aggregates when adding the surfactant or changing the temperature, we performed DLS experiments. We measured the hydrodynamic radius, R_H, at four scattering angles, θ = 30, 60, 90 and 120°. First, values of R_H, as a function of temperature, for the polyelectrolyte alone were obtained. A sharp transition temperature, LCST, of 38 ± 2 °C, with R_H going from about 1000 nm, below the LCST, to 350 nm, above it, was found (see Fig. SM-4a). In these samples the correlation functions were well fitted with cumulants (at least in the time range explored, see Fig. SM-3) and the characteristic diffusion times were found to depend linearly with q^2. Fig. 4 presents the hydrodynamic radius, R_H as a function of DTAB concentration, for two temperatures, above and below the transition temperature.

In the figure we observe that R_H decreases by a factor of about 4 as T becomes higher than the LSCT for all mixtures with $c_s < 0.5$ mM. For $0.5 < c_s < 2.8$ mM the change in R_H when T crosses the transition temperature, diminishes continuously, and becomes very small at a surfactant concentration of 2.8 mM. For concentrations higher or equal to 2.8 mM, the opposite is true, R_H increases as the temperature goes from 25 to 45 °C. We also observe that the collapse produced by the addition of surfactants at concentrations over 1.6 mM, at the lower temperature, is equivalent to the collapse produced on the free surfactant polymer solution at temperatures above the LCST. The polymer collapse at $c_s \sim 1$ mM is also observed by viscosity measurements (see Fig. SM-5).

The polydispersity index (PDI) obtained from cumulants analysis of the intensity auto-correlation functions, are between 0.05 and 0.3 for all samples with $c_s \geq 1.6$ mM. For free DTAB Cop-L solutions and mixtures with $c_s < 1.6$ mM at T = 25 °C, the obtained PDI were between 0.5 and 1, in those cases we used CONTIN analysis. For the same solutions but at T > LCST, the PDI were below 0.3.

For each surfactant concentration, the hydrodynamic radius as a function of temperature was also measured by DLS. In Fig. SM-4 in the supplementary material, we show the change in R_H as the temperature increases for the Cop-L solution with $c_p = 400$ mg L^{-1} and for the mixed system with 2.8 mM of DTAB. In the first case (Fig. SM-4a) R_H diminishes abruptly from about 1300 to 300 nm when the transition temperature is crossed. This was the system with the maximum change in size, being the relative change in size of around −77% (size decrement). The minimum variation of R_H was found for the system with 2.8 mM of DTAB (Fig. SM-4b), which presented a relative change in size of +20% (size increase). We recall that for all systems with $c_s > 2.8$ mM, the hydrodynamic radius increases as T becomes higher than the transition temperature (see Fig. 4).

3.5. Surface compression viscoelasticity

It is generally accepted that the dynamics and stability of emulsions and foams depend strongly on the surface compression surface elasticity [36,37]. In Fig. 5 we present the results for the surface compression viscoelasticity corresponding to the mixture Cop-L ($c_p = 400$ mg L^{-1}) + DTAB ($c_s = 1.6$ mM) measured at 25 and 45 °C. The real, E′, and imaginary, E″, parts of the complex surface compression modulus are shown in the same figure and for both temperatures. We recall here that E′ is the storage modulus which describes the elastic response of the system, and E″ is the loss modulus, which is equal to the product of surface compression viscosity and the angular frequency.

The results corresponding to the mixtures with 0.3 and 2.8 mM of DTAB are shown in the supplementary material (Figs. SM-6 and SM-7). We note that, for $c_s < 2.8$ mM, up to three relaxation times are present (see Fig. SM-8) while for the mixture with $c_s = 2.8$ mM, only one relaxation time was found. The origin of these relaxations is unclear, it could be related to the adsorption/desorption dynamics of soluble species or to the 2D dynamics of complexes irreversible adsorbed to the interface.

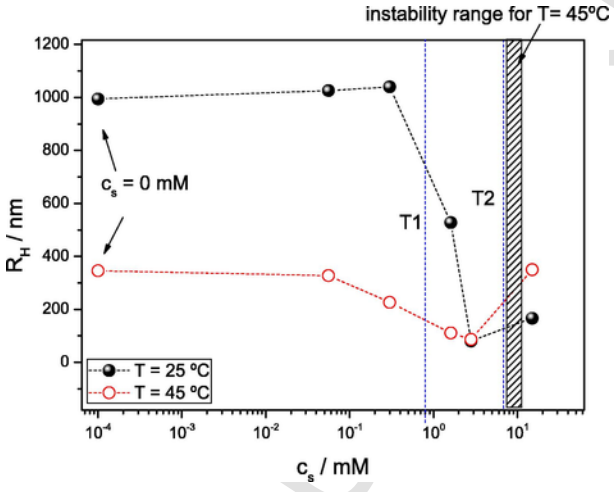

Fig. 4. Hydrodynamic radius of Cop-L/surfactant complexes in aqueous solution, $c_p = 400$ mg L^{-1}, as a function of DTAB concentration at 25 °C (closed circles) and at 45 °C (open circles). The points corresponding to Cop-L 400 mg L^{-1} without surfactant are included out of scale ($c_s = 0$).

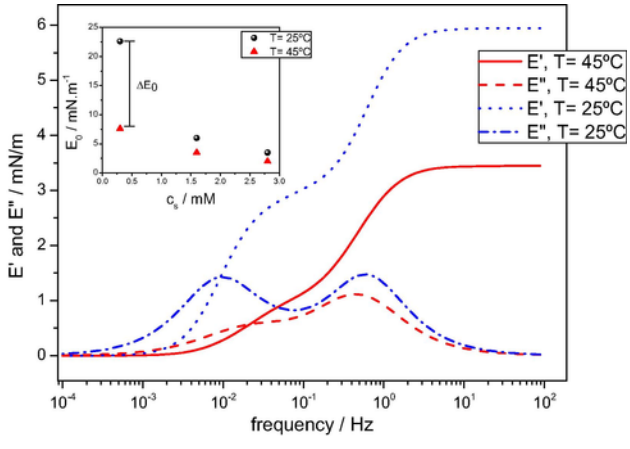

Fig. 5. Storage (elastic) and loss (viscous) compression modulus obtained from step-compression experiments (see SM). Results correspond to Cop-L 400 mg L^{-1} + DTAB 1.6 mM. More results on supporting information. The inset shows the high frequency limit of the elasticity, E_0, as a function of DTAB concentration.

In all cases, the elastic modulus, E′ is larger for the lower temperature and lower surfactant concentration. The surface loss (viscosity) modulus displayed a similar behavior.

In the inset of Fig. 5 the values for the high frequency limit of the elasticity are plotted as a function of the surfactant concentration for both temperatures. Note that the change in the high frequency limit of the elasticity, ΔE_0 in the figure, diminishes with c_s as T goes from 25 to 45 °C.

3.5.1. Foam stability and dynamics

Our original interest in this complex polymer/surfactant system was because of the possibility of using it to produce thermoresponsive foams. In light of Fig. 4 we chose to study foams stabilized with solutions at a fixed polymer concentration of 400 mg L^{-1} and mixed with DTAB at surfactant concentrations of 0.3; 1.6; 2.8 and 20 mM, in an attempt to find a correlation between foam stability and structural changes. Recall that at 0.3 and 1.6 mM there is a reduction in the size of the aggregates (see Fig. 4) when T goes over the transition temperature, while for c_s = 2.8 mM and c_s = 20 mM there is an increment in the aggregate's sizes (see Fig. 4 and SM-4) when T crosses the LCST. In the experiments that follow the initial liquid fraction for all foams was fixed to ϕ_l = 0.25 and the mean initial bubble radius, R_B, was about 70 μm.

In Fig. 6a an example of a plot of the relative light intensity transmitted through the foam sample as a function of time is shown. The relative intensity is defined as: $I\text{-}I_0/I_{final}$, being I, I_0 and I_{final} the instantaneous, I(t), initial, I(t=0) and final (without foam) transmitted light intensities respectively. Because the optical fiber is placed at the middle of the foam container, the time at which the relative intensity reaches a value of 1 indicates the moment when the foam sample (foam + liquid drained) has half its initial height, and the corresponding time, $t_{1/2}$, indicated by arrows in Fig. 6a, is a measure of foam stability. In Table 1 we present all results for $t_{1/2}$ at both temperatures,

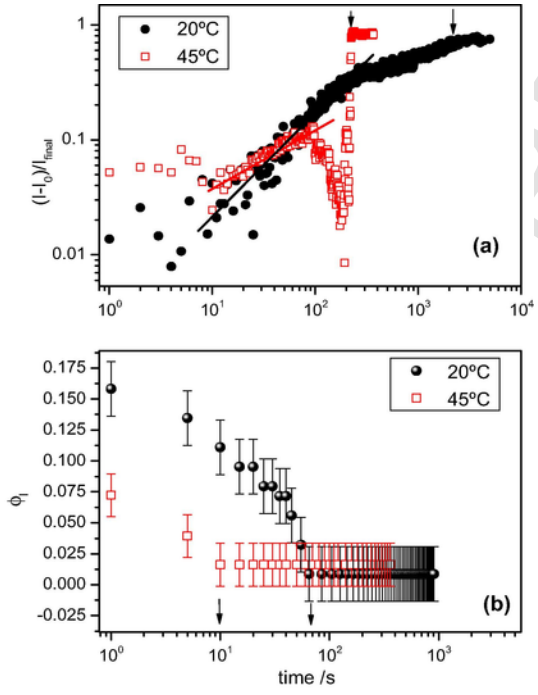

Fig. 6. Light intensity (a) and liquid fraction (b) as a function of time for a Cop-L/DTAB mixture: Cop-L 400 mg L^{-1} + DTAB 1.6 mM.

Table 1
Foam stability measured by the time needed to reach half the initial foam height, $t_{1/2}$. 20* indicates the free polymer surfactant solutions. The polymer concentration for all measurements was c_p = 400 mg L^{-1}. The time is given in seconds. All results are the mean values of several experiments on the same systems.

[DTAB] (mM)	$t_{1/2}$ (20 °C) (s)	$t_{1/2}$ (45 °C) (s)	$t_{1/2}$ (20 °C)/$t_{1/2}$ (45 °C)
20*	500	195	~2.6
20	1850	100	~18
2.8	1000	180	~5
1.6	2000	200	~10
0.3	3250	300	~11

including the results obtained for free polymer DTAB solutions of c_s = 20 mM (labelled as 20*) that we use for comparison.

From Table 1, we note that for all the mixtures, the foams are more stable at T = 20 °C than at T = 45 °C, even more, for the mixed systems with DTAB concentrations of c_s = 1.6, c_s = 0.3 and c_s = 20 mM, the foam stability at the lower temperature is between 10 and 18 times higher. The most stable foam was obtained for c_s = 0.3 mM for which $t_{1/2}$ turned to be about 54 min (average value over 10 independent measurements). For all foams at T > LCST, we observed that bubble collapse produces large holes inside the foam volume, this can be seen in Fig. 6a in the oscillations of the light intensity for the measurement at T = 45 °C (see also images in supporting information). Once the bubbles start to collapse, all the foam is destroyed rapidly in a cooperative process (cascades of bubble ruptures is what we observe in Fig. 6a for 100 < t < 200 at T = 45 °C, red squares).

In Fig. 6a we also note that the transmitted light intensity varies, in the log-log plot, linearly with time, in the region 10 < t < 100 s, at both temperatures. The linear fits give $I \sim t^{(0.93\pm0.2)}$ and $I \sim t^{(0.53\pm0.1)}$ for T = 20 and 45 °C respectively. We also observe a change in the slope at about t = 300 s for the system at T = 20 °C, in this case the fit gives $I \sim t^{(0.3\pm0.1)}$ (for 300 < t < 3000 s). At t > 300 s we observed on the wall of the foam container, that some bubbles rupture but the process does not produce cascades of events as occurs at T = 45 °C.

In Fig. 6b, results of free drainage experiments on the same sample are presented. The volume of the liquid drained was followed by direct observation with a CCD camera as a function of time. Note that the drainage is faster for T = 45 °C than for T = 20 °C, being the drainage characteristic time (arrows in Fig. 6b) about 6 times larger for T = 20 °C than for T = 45 °C. For other surfactant concentrations the drainage velocity is 3–10 times larger at 45 than at 20 °C, the smaller difference corresponding to c_s = 2.8 mM.

4. Discussion

4.1. Phase behavior, dynamic light scattering and equilibrium surface tension

The behavior of aqueous solutions of polyelectrolyte-oppositely-charged surfactant mixtures depends on the specific chemical system [38]. Their bulk phase behavior as well as its relation with the properties at the solution-air interface are often complicated by non-equilibrium effects, particularly, we can observe the appearance of peaks in the surface tension isotherms when the system enters the equilibrium two-phase region, which occurs close to charge neutralization [26,38,39]. Far from this region, the polyelectrolyte-surfactant complexes form an equilibrium one-phase solution or remain trapped in non-equilibrium kinetically arrested states forming a stable colloidal dispersion, which is possible only because the complexes retain enough charge to maintain colloidal stability. For our mixtures, from the absence of surface tension peaks, from the ζ-potential results (see

SM) and keeping in mind that two protocols of mixing were employed without observing any difference in the obtained results (see methods), it seems that the Cop-l/DTAB mixtures are not complicated by non-equilibrium effects, at least for the concentrations used and in the time scale of our experiments and particularly for T = 25 °C. Thus, in order to interpret the equilibrium surface tension results, let us use the following oversimplified picture [40–43]: When an oppositely charged surfactant is added to a polyelectrolyte solution it first progressively replaces the polyelectrolyte counterions in the vicinity of the macromolecular main chain. Generally, this process does not conduct to observable changes in the bulk properties of the system which could be followed with commonly used techniques such as conductivity or light scattering, however they can be detected by more sensitive, and less common techniques such as Electric birefringence [44]. This situation changes when a certain surfactant concentration, the critical aggregation concentration (*cac*), is reached. At this concentration, surfactant molecules begin to cooperatively bind onto the macromolecule chain. The *cac*, in general, occurs at concentrations 1–3 orders of magnitude lower than the *cmc* of pure surfactant solutions, and can be determined by surface tension [38] measurements, as shown in Fig. 2. From said figure we identified three characteristic surfactant concentrations: T1, T2 and T3. The concentration T1, which corresponds to the beginning of the first plateau, is generally associated to the *cac* [45] and corresponds to the onset of binding of DTAB to alginate-g-PNIPAAm in bulk. Upon further increase of the amount of surfactant, the polymer saturation point (T2) is reached. At this point, it is assumed that surfactant molecules occupy all of the binding sites of the polymer and that any excess causes a decrease in surface tension until the *cmc* is reached. Note that the concentration T2 (~7 mM) is below the concentration at which the electrophoretic mobility approaches zero (~15 mM at 25 °C, see results on Fig. SM-9), which is close to T3. Above T3, any DTAB addition would lead to the formation of micelles probably decorated with polymer chains, with no effect on surface tension [46]. Besides the overall decrease in surface tension previously mentioned, the temperature increment seems to cause a slight shift of T1, probably due to an increased hydrophobicity interaction between polymer and surfactant. Also, in contrast to the behavior observed at 25 °C, at 45 °C the polymer precipitated in a concentration region between 8 and 15 mM, i.e. between T2 and T3, this is also attributed to the increased hydrophobicity of the aggregates at the higher temperature. At concentrations above T3, the precipitates are redissolved, leading to stable dispersions. This last concentration coincides with the *cmc* of the surfactant (*cmc* ~ 15 mM at T = 25 °C and *cmc* ~ 16 at T = 45 °C respectively [47]) and also with the surfactant concentration region where a size increment is observed as T increases over the transition temperature (see DLS data), thus we interpret this as indication of a change in the structure of the aggregates in bulk.

The effect of DTAB and temperature at the interface is clearly seen in Fig.3. For pure liquids, the slopes of the surface tension vs. temperature curves are related to the surface entropy, $S^s = -\frac{\partial \gamma}{\partial T}$, and therefore, the changes in the slopes, m ($m = \frac{\partial \gamma}{\partial T}$, from Fig. 3) can be related to changes in the surface entropy. The relative changes in the slopes, m_r when the transition temperature is crossed are shown in Fig. 7 as a function of DTAB concentration. The relative slope change, m_r is defined as,

$$m_r = \frac{m_{T<LCST} - m_{T>LCST}}{m_{T<LCST}} \quad (5)$$

where $m_{T<>LCST}$ stands for the slopes below (<) and above (>) the

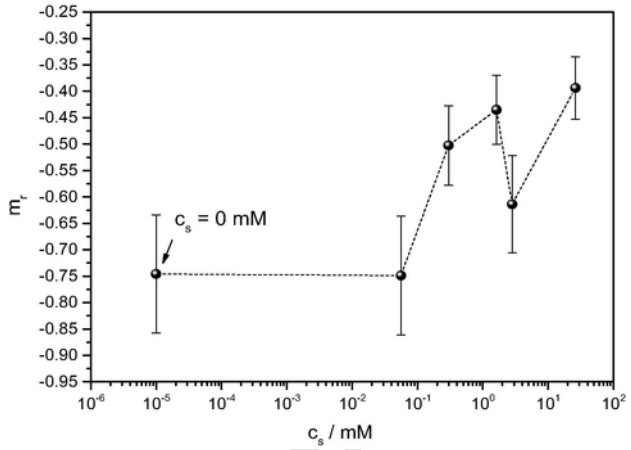

Fig. 7. Relative change of slopes of surface tension vs. T curves when crossing the transition temperature at each surfactant concentration as obtained from Fig. 3.

LCST. For free surfactant polyelectrolyte solutions, the reduction of the slope is about 75%, suggesting an entropy reduction as T becomes higher than the transition temperature. This can be rationalized in terms of the conformational changes occurring on the polymer chains, which go from coil to globule, at the interface. As the DTAB concentration increases, it induces a progressive collapse of the polyelectrolyte at temperatures below the LCST (see Fig. 3) then, the conformational changes observed when crossing the transition temperature are less and less pronounced. This is what we observe from the relative changes in the slopes shown in Fig. 7. Note that this behavior is consistent with the reduction in sizes observed in bulk, the entropy change seems to correlate well with the relative change in sizes measured by DLS (see Section 3.4). This also correlate well with the decrement on foam responsiveness as c_s increases.

The results of DLS are similar to those found for DTAB/CarboxyMC (sodium corboxymethylcellulose) [48]. The addition of an oppositely charged surfactant to a flexible polyelectrolyte produces, at certain concentrations, the polymer collapse. The polydispersity indexes measured (PDI < 0.3) indicate the formation of quite monodisperse aggregates both when $c_s > 1.6$ mM at low temperature, and for T > LCST at all surfactant concentrations. As stated in reference [48] the monodispersity of the aggregates is quite surprising if ones takes into account the rather broad size distribution of the polyelectrolyte chain.

Fig. 4 clearly shows that the addition of DTAB produces, at $c_s = 2.8$ mM, a hydrophobic collapse of the polymer chain in a way similar to that produced by increasing T above the LCST for Cop-L solutions without DTAB. This collapse of the polymer chain as the DTAB concentration increases is also observed by viscosity measurements (Fig. SM-5).

The increase in aggregate size after the collapse, as DTAB concentration increases, was also observed in the DTAB/carboxilMC system. This suggests a change in the structure of the aggregates as c_s increases above T2 (Fig. 4), probably because of the presence of surfactant micelles.

4.2. Surface compression viscoelasticity and foam stability

When studying foams stabilized by mixtures of polyelectrolytes and surfactants a very complex picture emerges. At first glance it seems that no straightforward connection between composition and structure of aggregates in bulk, surface properties (such as surface elasticity), foams films features (thicknesses, disjoining pressure) and

macroscopic foam stability exists [7,39,49–57]. However, regarding the tunability of foam stability in general, and in order to formulate responsive foams, two approaches can be found in the literature, each using a different mechanism of foam destabilization. In one, external stimuli are used to modify the bulk properties (e.g. viscosity) within the liquid films and channels between adjacent bubbles, in order to tune the foam stability (see Ref. [8] and references therein). In the second approach to tune foam stability by means of external stimuli, the mechanism of foam destabilization involves a direct modification of the interfacial layer adsorbed at the gas-liquid interface of bubbles. An example of this are foams stabilized by AzoTaB, a photoresponsive surfactant, whose stability changes when illuminated with different light intensities and wavelengths [11,58].

We are trying to elucidate the mechanism involved in the switching of foam stability when T changes and its dependence with surfactant concentration. Let us discuss first if a bulk mechanism could be at play in the aging process for the Cop-L/DTAB system. First, changes in the structure of the aggregates induced by temperature and surfactant concentration could modify the bulk viscosity, which in turn could affect the foam dynamics, for instance it could speed-up or slow down the drainage velocity, changing the stability of the foam. We performed measurements of relative viscosity, $\eta_{solution}/\eta_{water}$, in the Cop-L/surfactant mixtures as a function of DTAB concentration (see Fig. SM-5) and we observed that the maximum change of bulk viscosity occurred for free surfactant polymer solutions, for which the viscosity changed by a factor of 1.2 when the temperature went from 45 to 25 °C. The effect of temperature on the bulk viscosity is small and thus, it seems that it is not what controls the foam stability. Additionally, and with respect to drainage dynamics, the process is faster for T > LCST thus, one could think that the changes in the size of the aggregates which take place inside the confined media given by liquid channels between bubbles, when the temperature crosses the LSCT, could explain the observed changes in drainage times and foam stability. In this respect, we can estimate the size of the Plateau borders (liquid channels between adjacent bubbles) [59],

$$r_{PB} = \sqrt{\phi_l R_B^2} \tag{9}$$

being r_{PB} the Plateau border radius. For our foams, $R_B = 70\,\mu m$ and $\phi_l = 0.25$ for the initial stage of the free drainage process, thus, from Eq. (9), $r_{PB} = 35\,\mu m$, this is 35 times larger than the larger aggregate size ($R_H \sim 1\,\mu m$). For the final stage of the drainage process $\phi_l = 0.02$, $r_{PB} > 10\,\mu m$ which is ten times the larger aggregate hydrodynamic radius (note that because of coarsening, R_B will be larger than the initial value of 70 μm). Additionally, the final (stationary) liquid fraction is almost the same at both temperatures (~2%, see Fig. 6), these results seem to indicate that some other mechanism is involved in the destabilization of the foams when T crosses the LSCT.

Thus, for foams stabilized with Cop-L/DTAB mixtures, we believe that the mechanism of destabilization is probably linked to interfacial processes. From Figs. 2, 3 and 7, we saw that temperature has an effect on the equilibrium surface tension, however said figures also show that the equilibrium surface tension cannot be responsible for the change in stability in the high temperature regime. Another possible explanation of the change in foam stability when T > LCST, is that there is a modification of surface rheology as T crosses the LCST. In Fig. 6 (and also in Fig. SM-6) it is evident that the compression elasticity indeed changes, by a factor of about 3, when T crosses the LCST which could be related to the change in foam stability. Coalescence, the fusion of two bubbles after the rupture of the liquid film between them, is commonly thought to be caused by one of two possible mechanisms of film rupture. The first model considers the rupture as a consequence of thermal thickness fluctuations [60], the amplification of such fluctuations conducting to a rupture depending on parameters such as the surface tension and disjoining pressure (force per unit area between the two sides of the liquid film [1]. The second model considers the formation of interfacial regions where the surfactant is depleted ("holes") produced by thermal fluctuations. De Gennes proposed that the nucleation characteristic time for the holes should vary exponentially with the compression elastic modulus and he expressed the lifetime of foam films, τ_c as [6,61],

$$\tau_c \sim \exp\left(\frac{E_0 a}{k_B T}\right) \tag{10}$$

Being *a* the area occupied by surfactant molecules at the interface and E_0 the compression elastic modulus in the high frequency limit. Even though Eq. (10) is valid for thermal fluctuations in isolated single liquid films, one would expect the formation of more stable foams for systems with large surface elastic modulus, as observed in our systems. Note that the mixtures with $c_s = 0.3$, for which E_0 is the largest (Fig. SM-6), produced the more stable foams (Table 1).

From the surface compression rheology results, it is clear that the collapse of the polymer chain induced either by the surfactant concentration or the temperature has an effect on the surface elasticity. We recall that the change in the high frequency limit for the elasticity as T changes, is larger for the smallest c_s (see inset of Fig. 5) and diminishes as c_s increases, being this well correlated with the tuneability of the foams with temperature (Table 1).

It was also suggested, from theoretical models and numerical calculations, that for insoluble or irreversible adsorbed monolayers, coarsening dynamic is also influenced by compression elastic modulus [62,63] in the low frequency region [36,37]. In this respect, the temporal dependence of the light transmitted through the foam samples, as shown in Fig. 6, could be used, under certain conditions and for constant liquid fraction, to follow the coarsening dynamics [64–66]. The transmitted light intensity I(t), is proportional to the photon transport mean free path, L^*, which is proportional to the mean bubble diameter, thus $I(t) \sim L^* \sim R_B(t)$ [64]. For three-dimensional foams, it was shown that coarsening dynamics follow power laws, $R \sim t^z$, being $z = 1/3$ and $z = 1/2$ for wet and dry foams respectively [67]. In Fig. 6a we saw that the time evolution of the light intensity follows a power laws (lines shown in the log-log plot, Fig. 6) for certain time ranges. However, in these experiments the temporal evolution of the light intensity could depend simultaneously on drainage, coarsening and coalescence dynamics, and thus the observed behavior cannot be assigned exclusively to the coarsening rate. Let us examine the results of Fig. 6 more closely. First please note that the drainage process is finished in about 10 s for the foams at T = 45 °C (Fig. 6b). For t between 10 and 100 s the power law, $I \sim t^{0.52}$, has an exponent which is very close to 1/2, corresponding to the scaling expected for coarsening in 3D dry foams. That is why we believe that the observed time dependence of the light intensity corresponds, in this case, to the coarsening dynamics. However, because we haven't measured the bubble size distribution as a function of time experimentally, in order to verify that the self-similar regime of coarsening is reached and maintained during the light intensity measurements, some coalesce could be present. For these foams, and for t > 100 s, cascades of bubble coalescence and collapse are observed, producing large holes and destroying the entire foam rapidly. As stated, this behavior can be observed in the oscillations of the intensity of light

(Fig. 6a, red squares) at t ~ 200 s (see also pictures in the supporting material).

In the case of foams at 20 °C, the drainage process is present up to t = 80 s, the power law being $I(t) \sim t^{0.93}$ and holding for $10 < t < 300$. It is impossible to separate the contributions due to coarsening and drainage in this case. For times larger than 100 s, the stationary liquid fraction was attained (compare time scales in Fig. 6b and a) but for about 100 s more, the power law holds with the same exponent. During this period the liquid fraction is constant and no appreciable coalescence was observed on the walls of the foam container. Thus, one could think that, for $80 < t < 300$, the variation of I vs t is caused mainly by coarsening. The time dependence of light intensity changes slope at t ~ 300 s and I(t) follows a power law with exponent equal to 0.3. An exponent of 1/3 is what one would expect for coarsening in wet foams, however, this cannot be the case because the liquid fraction is about 2% and equal (or even lower) to that of foams at 45 °C. At this stage of the aging process of the foam, we observed coalescence but the dynamic observed was not cooperative (cascades), as was observed at T = 45 °C, but continuous.

Summarizing, in the time periods where we could think that the time dependence of the light intensity corresponds to the coarsening process, the scaling shows that it is faster for T = 20 °C ($\sim t^{0.9}$) than for T = 45 °C ($\sim t^{0.5}$). Because the coalescence dynamics are produced in a continuous manner for T = 20 and in a cooperative process (cascades) for T = 45 we conclude that the differences in foam stability as T goes over the LSCT, are due to the different coalescence and collapse dynamics. In this respect, if an avalanche of events is produced after the rupture of a liquid film, it is likely due to the mechanical perturbation produced by said rupture on adjacent films and bubbles. Since this perturbation is mainly dilational in nature, bubbles should be more capable of resisting rupture when the liquid films have high surface compression elasticities.

From all these results, we are driven to conclude that the stability of the foams would be controlled by the surface compression elasticity in the high frequency region. This depends on the conformation of the co-polyelectrolyte, which in turn depends on surfactant concentration and the temperature. The ability of switching the stability of the foams with T would result from the relative change in E_0 when T crosses over the LCST, if E_0 falls below a certain threshold a single bubble rupture can trigger an avalanche of ruptures that destroy the entire foam.

At the same time, surface compression viscosity could play a role in the process of collapse by dissipating energy and affecting the cooperativity of the rupture dynamics, in a manner similar to that observed for 2D foams with bulk viscosity [68], however, the reader should note that the effects produced on the surface loss moduli when T goes over the LCST are not very pronounced (see Fig. 6 and SM-6 and SM-7).

Another possible destabilization mechanism of the foams at T > LSCT should be considered. When the temperature goes over it's critical value, very hydrophobic globules are formed which could act as antifoaming particles and produce the film rupture via a bridging mechanism [69]. However, because the foaming behavior at T = 45 °C is not very different from that at T = 20 °C (same volumes of foams produced with the same number of syringes cycles), this mechanism should not come into play. Finally, although we did not measure shear surface elasticity and viscosity, they could be involved in the stabilization/destabilization of our foams. Surface viscosity surely plays a role in the differences observed in the drainage dynamics [5,70].

5. Conclusions

Previous efforts to produce thermoresponsive foams using mixtures of the uncharged polymer PNIPAAM and surfactants failed because the surfactant molecules displace the PNIPAAM from the interface [17], removing the thermoresponsiveness. Because of this, we hypothesized that thermoresponsive foams could be formulated with aqueous mixtures of a cationic surfactant and a brush-type anionic polyelectrolyte, incorporating the PNIPAAm as side chains. We hypothesized that the oppositely charged surfactant would act as an anchor to the interface for the polyelectrolyte, retaining the thermoresponsiveness at the interface and, at the same time, improving the foamability and stability of the foams. We synthetized a new graft "co-polyelectrolyte" with a brush-type structure based on alginate, a negatively charged polyelectrolyte, with PNIPAAm as side chains, and used it mixed with DTAB, a cationic surfactant, to stabilize foams. We found that stimulable stable foams could in fact be formulated but only in a very narrow range of surfactant concentrations, $0.3 \leq c_s \leq 1.6$ mM. At surfactant concentrations below this range, the foams were not stable enough to be studied and at higher DTAB concentrations the responsiveness was lost and the foam stability diminished. At temperatures below the LCST the reduction of the thermoresponsiveness due to the increment of the surfactant concentration is a consequence of conformational changes produced in the co-polymer chain as DTAB molecules bind to it. The polyelectrolyte-DTAB aggregates became more and more hydrophobic promoting the chain collapse at all temperatures, in this collapsed state the aggregate cannot respond to temperature changes (see Fig. 8).

The changes in aggregate structures and sizes at the interface produce modifications on the surface rheology, particularly on surface compression elasticity. Although more work is needed to clarify the mechanism of stabilization/destabilization of foams formulated with polyeletrolyte-surfactant mixtures and no straightforward links between surface properties and foam stability exist in the literature [7,39,49–57], all the experimental evidence we have, even though incomplete, seems to support the idea that changes in the high frequency compression elasticity, even if small, are the cause of the responsiveness of the studied foams via the coalescence dynamics: if modifying the temperature, E_0 falls below a certain threshold, a single bubble rupture can trigger an avalanche of ruptures that destroy the entire foam. A clear correlation between surface dilational elasticity (and film thickness) and foam stability was reported very recently in a polyeletrolyte/surfactant system formed by NaPSS and CTAB [49]. However, because other mechanisms, such as defoaming by bridging [69], could be at play and in order to clarify the mechanism involved in the stabilization/destabilization of foams formulated with these systems, a systematic study correlating conformational changes in bulk and at surfaces with film thickness, surface shear and dilational viscoelasticity and their relations with coarsening and coalescence dynamics, as well as with the occurrence of cooperative phenomena, such as avalanches of bubble ruptures [59,68,71] or topological changes[72], is needed.

To the best of our knowledge, this is the first system based on derivatives of PNIPAAm successfully used in the formulation of thermoresponsive foams. A clear advantage of these systems, as some others [73], is that the response can be achieved at a quite low temperature (~38 °C) compared to other thermoresponsive systems [12].

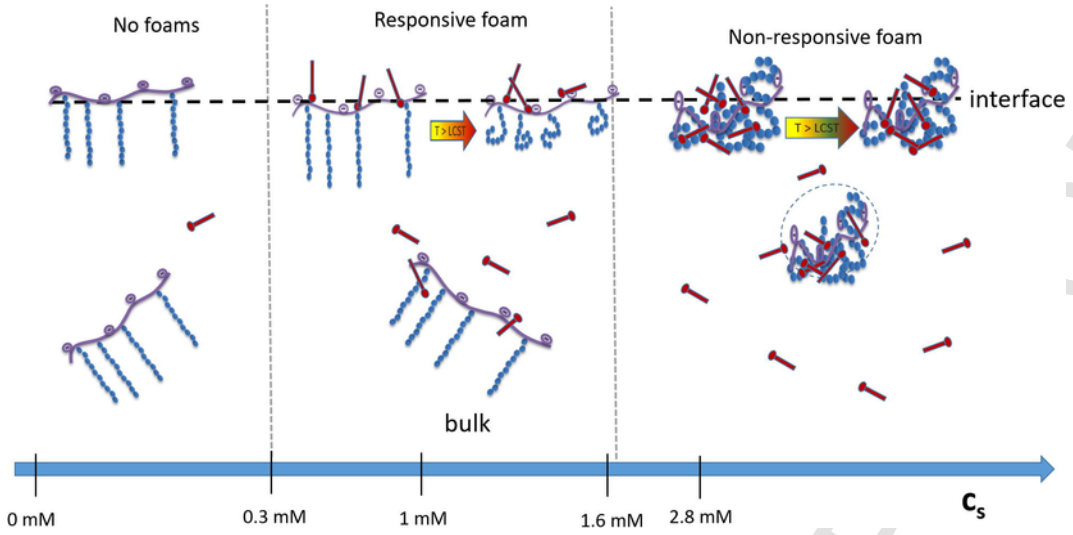

Fig. 8. Schematic representation of ideas outlined on the conclusions. The foam responsiveness is lost if the copolymer is in its collapsed state due to surfactant aggregation, this happens at $c_s \geq 1.6$ mM.

Acknowledgements

We thank Dominique Langevin for proofreading the manuscript and for valuable scientific discussions. This work was partially supported by grants PGI-UNS 24/F067 of Universidad Nacional del Sur and PICT 2013 (D) Nro 2070 and PICT 2016 Nro 0787 of Agencia Nacional de Promoción Científica y Tecnológica (ANPCyT) and PIP-GI 2014 Nro 11220130100668CO (CONICET). CD and EFM thank CONICET for their fellowships. HR thanks MFF and NR.

Appendix A. Supplementary material

Supplementary data associated with this article can be found, in the online version, at https://doi.org/10.1016/j.jcis.2017.10.090.

References

[1] D. Langevin, Aqueous foams: a field of investigation at the Frontier between chemistry and physics, ChemPhysChem 9 (2008) 510–522.
[2] D.L. Weaire, S. Hutzler, The Physics of Foams, Clarendon Press, Oxford New York, 1999.
[3] D.R. Ekserova, P.M. Krugliakov, Foam and Foam Films: Theory, Experiment, Application, first ed., Elsevier Science B.V, Amsterdam, 1998. doi: 10.1016/S1383-7303(98)80004-5.
[4] C. Hill, J. Eastoe, Foams: from nature to industry, Adv. Colloid Interface Sci. 247 (2017) 496–513, https://doi.org/10.1016/j.cis.2017.05.013.
[5] A. Saint-Jalmes, Physical chemistry in foam drainage and coarsening, Soft Matter. 2 (2006) 836, https://doi.org/10.1039/b606780h.
[6] D. Langevin, Bubble coalescence in pure liquids and in surfactant solutions, Curr. Opin. Colloid Interface Sci. 20 (2015) 92–97, https://doi.org/10.1016/j.cocis.2015.03.005.
[7] A. Bureiko, A. Trybala, N. Kovalchuk, V. Starov, Current applications of foams formed from mixed surfactant-polymer solutions, Adv. Colloid Interface Sci. 222 (2014) https://doi.org/10.1016/j.cis.2014.10.001.
[8] A.-L. Fameau, A. Carl, A. Saint-Jalmes, R. von Klitzing, Responsive aqueous foams, Chemphyschem 16 (2015) 66–75, https://doi.org/10.1002/cphc.201402580.
[9] A. Carl, R. von Klitzing, Smart foams: new perspectives towards responsive composite materials, Angew. Chemie Int. Ed. 50 (2011) 11290–11292, https://doi.org/10.1002/anie.201105399.
[10] S. Fujii, Y. Nakamura, Stimuli-responsive bubbles and foams stabilized with solid particles, Langmuir 33 (2017) 7365–7379, https://doi.org/10.1021/acs.langmuir.7b01024.
[11] E. Chevallier, A. Saint-Jalmes, I. Cantat, F. Lequeux, C. Monteux, Light induced flows opposing drainage in foams and thin-films using photosurfactants, Soft Matter 9 (2013) https://doi.org/10.1039/c3sm50258a.
[12] A.-L. Fameau, A. Saint-Jalmes, F. Cousin, B. Houinsou Houssou, B. Novales, L. Navailles, F. Nallet, C. Gaillard, F. Boué, J.-P. Douliez, Smart foams: switching reversibly between ultrastable and unstable foams, Angew. Chem. Int. Ed. 50 (2011) 8264–8269, https://doi.org/10.1002/anie.201102115.
[13] A.P.J. Middelberg, M. Dimitrijev-Dwyer, A designed biosurfactant protein for switchable foam control, ChemPhysChem 12 (2011) 1426–1429, https://doi.org/10.1002/cphc.201100082.
[14] A.F. Dexter, A.S. Malcolm, A.P.J. Middelberg, Reversible active switching of the mechanical properties of a peptide film at a fluid-fluid interface, Nat. Mater. 5 (2006) 502–506, https://doi.org/10.1038/nmat1653.
[15] L.T. Lee, B. Jean, A. Menelle, Effect of temperature on the adsorption of poly(N-isopropylacrylamide) at the air−solution interface, Langmuir 15 (1999) 3267–3272, https://doi.org/10.1021/la981531s.
[16] C. Monteux, R. Mangeret, G. Laibe, E. Freyssingeas, V. Bergeron, G. Fuller, Shear surface rheology of poly(N-isopropylacrylamide) adsorbed layers at the air−water interface, Macromolecules 39 (2006) 3408–3414, https://doi.org/10.1021/ma052552d.
[17] R.-M. Guillermic, A. Saint-Jalmes, Dynamics of poly-nipam chains in competition with surfactants at liquid interfaces: from thermoresponsive interfacial rheology to foams, Soft Matter 9 (2013) 1344–1353, https://doi.org/10.1039/C2SM26666K.
[18] V. Schmitt, V. Ravaine, Surface compaction versus stretching in Pickering emulsions stabilised by microgels, Curr. Opin. Colloid Interface Sci. 18 (2013) 532–541, https://doi.org/10.1016/j.cocis.2013.11.004.
[19] M.M.M. Soledad Lencina, Z. Iatridi, M.A. Villar, C. Tsitsilianis, Thermoresponsive hydrogels from alginate-based graft copolymers, Eur. Polym. J. 61 (2014) 33–44, https://doi.org/10.1016/j.eurpolymj.2014.09.011.
[20] T. Salomonsen, H.M. Jensen, F.H. Larsen, S. Steuernagel, S.B. Engelsen, Alginate monomer composition studied by solution- and solid-state NMR – a comparative chemometric study, Food Hydrocoll. 23 (2009) 1579–1586, https://doi.org/10.1016/j.foodhyd.2008.11.009.
[21] C.G. Gomez, M. Rinaudo, M.A. Villar, Oxidation of sodium alginate and characterization of the oxidized derivatives, Carbohydr. Polym. 67 (2007) 296–304, https://doi.org/10.1016/j.carbpol.2006.05.025.
[22] Y. Xia, X. Yin, N.A.D. Burke, H.D.H. Stöver, Thermal response of narrow-disperse poly(N-isopropylacrylamide) prepared by atom transfer radical polymerization, Macromolecules 38 (2005) 5937–5943, https://doi.org/10.1021/ma050261z.
[23] J.D. Debord, L.A. Lyon, Synthesis and characterization of pH-responsive copolymer microgels with tunable volume phase transition temperatures, Langmuir 19 (2003) 7662–7664, https://doi.org/10.1021/la0342924.
[24] R. Pamies, K. Zhu, A.-L. Kjøniksen, B. Nyström, Thermal response of low molecular weight poly-(N-isopropylacrylamide) polymers in aqueous solution, Polym. Bull. 62 (2009) 487–502, https://doi.org/10.1007/s00289-008-0029-4.
[25] H. Feil, Y.H. Bae, J. Feijen, S.W. Kim, Effect of comonomer hydrophilicity and ionization on the lower critical solution temperature of N-isopropylacrylamide copolymers, Macromolecules 26 (1993) 2496–2500, https://doi.org/10.1021/ma00062a016.

[26] I. Varga, R.A. Campbell, General physical description of the behavior of oppositely charged polyelectrolyte/surfactant mixtures at the air/water interface, Langmuir 33 (2017) 5915–5924, https://doi.org/10.1021/acs.langmuir.7b01288.
[27] C.D.D. Bain, P.M.M. Claesson, D. Langevin, R. Meszaros, T. Nylander, C. Stubenrauch, S. Titmuss, R. von Klitzing, Complexes of surfactants with oppositely charged polymers at surfaces and in bulk, Adv. Colloid Interface Sci. 155 (2010) 32–49, https://doi.org/10.1016/j.cis.2010.01.007.
[28] J.-F. Berret, G. Cristobal, P. Hervé, J. Oberdisse, I. Grillo, P. Hervé, J. Oberdisse, I. Grillo, Structure of colloidal complexes obtained from neutral/poly-electrolyte copolymers and oppositely charged surfactants, Eur. Phys. J. E – Soft Matter. 9 (2002) 301–311, https://doi.org/10.1140/epje/i2002-10063-7.
[29] D. Li, M.S. Kelkar, N.J. Wagner, Phase behavior and molecular thermodynamics of coacervation in oppositely charged polyelectrolyte/surfactant systems: a cationic polymer JR 400 and anionic surfactant SDS mixture, Langmuir 28 (2012) 10348–10362, https://doi.org/10.1021/la301475s.
[30] M. Štěpánek, J. Hajduová, K. Procházka, M. Šlouf, J. Nebesářová, G. Mountrichas, C. Mantzaridis, S. Pispas, Association of poly(4-hydroxystyrene)-block-poly(ethylene oxide) in aqueous solutions: block copolymer nanoparticles with intermixed blocks, Langmuir 28 (2012) 307–313, https://doi.org/10.1021/la203946s.
[31] K. Bodnár, E. Fegyver, M. Nagy, R. Mészáros, Impact of polyelectrolyte chemistry on the thermodynamic stability of oppositely charged macromolecule/surfactant mixtures, Langmuir 32 (2016) 1259–1268, https://doi.org/10.1021/acs.langmuir.5b04431.
[32] B. Miranda, H.M. Hilles, R.G. Rubio, H. Ritacco, D. Radic, L. Gargallo, M. Sferrazza, F. Ortega, Equilibrium and surface rheology of monolayers of insoluble polycations with side chains, Langmuir 25 (2009) 12561–12568, https://doi.org/10.1021/la901762u.
[33] P.J. Wilde, Interfaces: Their role in foam and emulsion behaviour, Curr. Opin. Colloid Interface Sci. 5 (2000) 176–181, https://doi.org/10.1016/S1359-0294(00)00056-X.
[34] Z. Briceño-Ahumada, W. Drenckhan, D. Langevin, Coalescence in draining foams made of very small bubbles, Phys. Rev. Lett. 116 (2016) 128302, https://doi.org/10.1103/PhysRevLett. 116.128302.
[35] W. Drenckhan, A. Saint-Jalmes, The science of foaming, Adv. Colloid Interface Sci. 222 (2015) 228–259, https://doi.org/10.1016/j.cis.2015.04.001.
[36] D. Georgieva, A. Cagna, D. Langevin, Link between surface elasticity and foam stability, Soft Matter 5 (2009) 2063, https://doi.org/10.1039/b822568k.
[37] D. Georgieva, V. Schmitt, F. Leal-Calderon, D. Langevin, On the possible role of surface elasticity in emulsion stability, Langmuir 25 (2009) 5565–5573, https://doi.org/10.1021/la804240e.
[38] E. Guzmán, S. Llamas, A. Maestro, L. Fernández-Peña, A. Akanno, R. Miller, F. Ortega, R.G. Rubio, Polymer–surfactant systems in bulk and at fluid interfaces, Adv. Colloid Interface Sci. 233 (2016) 38–64, https://doi.org/10.1016/j.cis.2015.11.001.
[39] L. Braun, M. Uhlig, R. von Klitzing, R.A. Campbell, Polymers and surfactants at fluid interfaces studied with specular neutron reflectometry, Adv. Colloid Interface Sci. 247 (2017) 130–148, https://doi.org/10.1016/j.cis.2017.07.005.
[40] L. Piculell, Understanding and exploiting the phase behavior of mixtures of oppositely charged polymers and surfactants in water, Langmuir 29 (2013) 10313–10329, https://doi.org/10.1021/la401026j.
[41] E.D. Goddard, K.P. Ananthapadmanabhan, Interactions of Surfactants with Polymers and Proteins, CRC Press, Boca Raton, 1993. doi: 10.1080/01932699408943565.
[42] Jan C.T. Kwak, Polymer-surfactant systems. Surfactant Science Series vol. 77, M. Dekker, New York, 1998.
[43] D. Langevin, Complexation of oppositely charged polyelectrolytes and surfactants in aqueous solutions. A review, Adv. Colloid Interface Sci. 147–148 (2009) 170–177.
[44] H.A. Ritacco, Electro-optic Kerr effect in the study of mixtures of oppositely charged colloids. The case of polymer-surfactant mixtures in aqueous solutions, Adv. Colloid Interface Sci. 247 (2017) 234–257, https://doi.org/10.1016/j.cis.2017.05.015.
[45] E.D.D. Goddard, Polymer/surfactant interaction: interfacial aspects, J. Colloid Interface Sci. 256 (2002) 228–235, https://doi.org/10.1006/jcis.2001.8066.
[46] O. Rac, P. Suchorska-Woźniak, M. Fiedot, H. Teterycz, Influence of stabilising agents and pH on the size of SnO_2 nanoparticles, Beilstein J. Nanotechnol. 5 (2014) 2192–2201, https://doi.org/10.3762/bjnano.5.228.
[47] M.T. Bashford, E.M. Woolley, Enthalpies of dilution of aqueous decyl-, dodecyl-, tetradecyl-, and hexadecyltrimethylammonium bromides at 10, 25, 40, and 55 °C, J. Phys. Chem. 89 (1985) 3173–3179, https://doi.org/10.1021/j100260a044.
[48] S. Guillot, D. McLoughlin, N. Jain, M. Delsanti, D. Langevin, Polyelectrolyte surfactant complexes at interfaces and in bulk, J. Phys. Condens. Matter. 15 (2003) S219–S224, https://doi.org/10.1088/0953-8984/15/1/328.
[49] F. Schulze-Zachau, B. Braunschweig, Structure of polystyrenesulfonate/surfactant mixtures at air-water interfaces and their role as building blocks for macroscopic foam, Langmuir 33 (2017) 3499–3508, https://doi.org/10.1021/acs.langmuir.7b00400.
[50] M. Uhlig, R. Miller, R. von Klitzing, Surface adsorption of sulfonated poly(phenylene sulfone)/C14TAB mixtures and its correlation with foam film stability, Phys. Chem. Chem. Phys. 18 (2016) 18414–18423, https://doi.org/10.1039/C6CP02256A.
[51] N. Kristen, A. Vüllings, A. Laschewsky, R. Miller, R. Von Klitzing, Foam films from oppositely charged polyelectolyte/surfactant mixtures: Effect of polyelectrolyte and surfactant hydrophobicity on film stability, Langmuir. 26 (2010) 9321–9327, https://doi.org/10.1021/la1002463.
[52] H. Ritacco, P.-A. Albouy, A. Bhattacharyya, D. Langevin, Influence of the polymer backbone rigidity on polyelectrolyte–surfactant complexes at the air/water interface, Phys. Chem. Chem. Phys. 2 (2000) 5243–5251, https://doi.org/10.1039/b004657o.
[53] C. Stubenrauch, R. von Klitzing, Disjoining pressure in thin liquid foam and emulsion films—new concepts and perspectives, J. Phys. Condens. Matter. 15 (2003) R1197–R1232, https://doi.org/10.1088/0953-8984/15/27/201.
[54] B.M. Folmer, B. Kronberg, Effect of surfactant-polymer association on the stabilities of foams and thin films: sodium dodecyl sulfate and poly(vinyl pyrrolidone), Langmuir 16 (2000) 5987–5992, https://doi.org/10.1021/la991655k.
[55] B. Kolarić, W. Jaeger, G. Hedicke, R.V. Klitzing, Tuning of foam film thickness by different (poly)electrolyte/surfactant combinations, J. Phys. Chem. B. 107 (2003) 8152–8157, https://doi.org/10.1021/jp0340358.
[56] H. Fauser, R. von Klitzing, Effect of polyelectrolytes on (de)stability of liquid foam films, Soft Matter 10 (2014) 6903–6916, https://doi.org/10.1039/c4sm01241k.
[57] R. Petkova, S. Tcholakova, N.D. Denkov, Foaming and foam stability for mixed polymer-surfactant solutions: effects of surfactant type and polymer charge, Langmuir 28 (2012) 4996–5009, https://doi.org/10.1021/la3003096.
[58] E. Chevallier, A. Mamane, H.A. Stone, C. Tribet, F. Lequeux, C. Monteux, Pumping-out photo-surfactants from an air–water interface using light, Soft Matter 7 (2011) 7866, https://doi.org/10.1039/c1sm05378g.
[59] E. Rio, A.L. Biance, Thermodynamic and mechanical timescales involved in foam film rupture and liquid foam coalescence, ChemPhysChem 15 (2014) 3692–3707, https://doi.org/10.1002/cphc.201402195.
[60] A. Vrij, Possible mechanism for the spontaneous rupture of thin, free liquid films, Discuss. Faraday Soc. 42 (1966) 23, https://doi.org/10.1039/df9664200023.
[61] P.G. De Gennes, Some remarks on coalescence in emulsions or foams, Chem. Eng. Sci. 56 (2001) 5449–5450, https://doi.org/10.1016/S0009-2509(01)00170-1.
[62] W. Kloek, T. van Vliet, M. Meinders, Effect of bulk and interfacial rheological properties on bubble dissolution, J. Colloid Interface Sci. 237 (2001) 158–166, https://doi.org/10.1006/jcis.2001.7454.
[63] M.B.J. Meinders, T. Van Vliet, The role of interfacial rheological properties on Ostwald ripening in emulsions, Adv. Colloid Interface Sci. 108–109 (2004) 119–126, https://doi.org/10.1016/j.cis.2003.10.005.
[64] D.J. Durian, D.A. Weitz, D.J. Pine, Scaling behavior in shaving cream, Phys. Rev. A 44 (1991) R7902–R7905, https://doi.org/10.1103/PhysRevA.44.R7902.
[65] M.U. Vera, A. Saint-Jalmes, D.J. Durian, Scattering optics of foam, Appl. Opt. 40 (2001) 4210, https://doi.org/10.1364/AO.40.004210.
[66] H. Ritacco, Playing with liquid foams: learning physical chemistry, J. Chem. Educ. 85 (2008) 1667–1669, https://doi.org/10.1021/ed085p1667.
[67] N. Isert, G. Maret, C.M. Aegerter, Coarsening dynamics of three-dimensional levitated foams: from wet to dry, Eur. Phys. J. E. 36 (2013) 116, https://doi.org/10.1140/epje/i2013-13116-x.
[68] H. Ritacco, F. Kiefer, D. Langevin, Lifetime of bubble rafts: cooperativity and avalanches, Phys. Rev. Lett. 98 (2007) 1–4, https://doi.org/10.1103/PhysRevLett. 98.244501.
[69] N.D. Denkov, Mechanisms of foam destruction by oil-based antifoams, Langmuir 20 (2004) 9463–9505, https://doi.org/10.1021/la049676o.
[70] W. Drenckhan, H. Ritacco, A. Saint-Jalmes, A. Saugey, P. McGuinness, A. van der Net, D. Langevin, D. Weaire, Fluid dynamics of rivulet flow between plates, Phys. Fluids 19 (2007) 1–12.
[71] N. Vandewalle, J.F. Lentz, S. Dorbolo, F. Brisbois, Avalanches of popping bubbles in collapsing foams, Phys. Rev. Lett. 86 (2001) 179.
[72] M. Durand, H.A. Stone, Relaxation time of the topological T1 process in a two-dimensional foam, Phys. Rev. Lett. 97 (2006) 226101, https://doi.org/10.1103/PhysRevLett. 97.226101.
[73] A. Salonen, D. Langevin, P. Perrin, Light and temperature bi-responsive emulsion foams, Soft Matter 6 (2010) 5308, https://doi.org/10.1039/c0sm00705f.